Available online at www.sciencedirect.com
ScienceDirect
Chemical Physics 347 (2008) 185–193
Chemical Physics
www.elsevier.com/locate/chemphys

Nonperturbative non-Markovian quantum master equation: Validity and limitation to calculate nonlinear response functions

Akihito Ishizaki *, Yoshitaka Tanimura

Department of Chemistry, Graduate School of Science, Kyoto University, Kyoto 606-8502, Japan

Received 1 September 2007; accepted 31 October 2007
Available online 22 November 2007

Abstract

Based on the influence functional formalism, we have derived a nonperturbative equation of motion for a reduced system coupled to a harmonic bath with colored noise in which the system–bath coupling operator does not necessarily commute with the system Hamiltonian. The resultant expression coincides with the time-convolutionless quantum master equation derived from the second-order perturbative approximation, which is also equivalent to a generalized Redfield equation. This agreement occurs because, in the nonperturbative case, the relaxation operators arise from the higher-order system–bath interaction that can be incorporated into the reduced density matrix as the influence operator; while the second-order interaction remains as a relaxation operator in the equation of motion. While the equation describes the exact dynamics of the density matrix beyond weak system–bath interactions, it does not have the capability to calculate nonlinear response functions appropriately. This is because the equation cannot describe memory effects which straddle the external system interactions due to the reduced description of the bath. To illustrate this point, we have calculated the third-order two-dimensional (2D) spectra for a two-level system from the present approach and the hierarchically coupled equations approach that can handle quantal system–bath coherence thanks to its hierarchical formalism. The numerical demonstration clearly indicates the lack of the system–bath correlation in the present formalism as fast dephasing profiles of the 2D spectra.

Keywords: Non-Markovian quatum master equation; Redfield equation; Quantum Fokker–Planck equation; Nonperturbative treatment; Nonlinear optical response function; Multidimensional spectroscopy

1. Introduction

Impressive progress in ultrafast spectroscopy has opened up real-time observation of molecular motion that has provided important tests for advancing the theoretical studies of quantum dynamics. Understanding condensed phase quantum dynamics is pivotal in elucidating diverse molecular processes such as vibrational relaxation, chemical reactions, electron or proton transfer, energy transfer in multichromophore complexes, and so forth. Hence, much effort is currently being devoted to the development of approaches for describing the quantum dynamics in these complex systems.

The great strides in computer power have enabled us to perform rigorous quantum dynamics calculations for small systems [1,2]. For systems with a large number of degrees of freedom, however, it is still extremely difficult to apply such calculations [3]. Thus, it is common that only the important degrees of freedom (*the relevant system*, or *the system*) are treated quantum mechanically, whereas the others (*the bath*) are treated classically. Unfortunately, the boundary between quantum and classical descriptions, which is set in an *ad hoc* fashion, may cause severe problems because the inherent effects of quantum interference cannot be treated appropriately [4–6].

Other commonly used approaches are based on the reduced equation of motion. In these approaches, the key quantity of interest is the reduced density matrix, i.e., the partial trace of the total density matrix over the bath degrees

* Corresponding author. Fax: +81 75 753 4018.
E-mail address: ishizaki@kuchem.kyoto-u.ac.jp (A. Ishizaki).

0301-0104/$ - see front matter © 2007 Elsevier B.V. All rights reserved.
doi:10.1016/j.chemphys.2007.10.037

of freedom. In contrast to the mixed quantum-classical methods, the reduced density matrix approach can describe the dynamics of the bath quantum mechanically. A considerable amount of research has been devoted to the construction of the equation of motion [7] e.g., the Nakajima-Zwanzig identity (the time-convolution quantum master equation) [8,9] the Shibata-Takahashi-Hashitsume identity (the time-convolutionless quantum master equation: TCL-QME) [10,11]. In most formulations, however, it is impossible to reduce explicit expressions for the equations beyond the exact formal structures. Hence, some approximations have to be invoked to make practical calculations possible. A well-known example is the Redfield equation, which invokes the perturbative approximation and the Markov approximation [12]. This equation has been applied to investigate the dynamics of electron-transfer [13–18] motion through conical intersections [19,20] photoisomerization [21,22] and energy transfer in multichromophore complexes [23,24] under the condition of weak system–bath coupling for which the second-order perturbative truncation should be valid. One approach to go beyond the restriction on the coupling strength is to include higher-order system–bath interaction terms [25–28]. However, the resultant expressions are quite cumbersome to treat. For the model of a linearly coupled harmonic oscillator bath, the path integral formalism provides a powerful alternative to perturbative approaches. The effects of the bath on the relevant system are described by the Feynman–Vernon influence functional [29] which allows us to handle strong system–bath coupling. Under the assumption of a white-noise bath (the Markov assumption), Caldeira and Leggett employed this formalism to derive a Markovian quantum master equation, which is sometimes referred as the quantum Fokker–Planck equation [30]. In order to include colored noise effects (non-Markovian effects), Tanimura and his coworkers constructed a set of hierarchically coupled equations of motion [31–36] by creating a fusion of the Caldeira-Leggett approach and Kubo's stochastic theory [37]. These equations employed the high-temperature approximation, and therefore cannot be applied to low-temperature systems. Thus, low-temperature correction terms for the hierarchical formalism were explored [38] and summarized as the closed hierarchy form as *the quantum Fokker–Planck equation with low-temperature correction terms (QFP-LTC)* [39–41].

In the present paper, we derive a reduced equation of motion in a nonperturbative manner with help of the influence functional formalism. Despite strenuous efforts to go beyond second-order perturbation, we have found that the present nonperturbative result is identical to the second-order perturbative approximation form of the TCL-QME as long as the bath is harmonic. This is because, in the nonperturbative case, the terms arise from the higher-order system–bath interaction that can be incorporated into the reduced density matrix as the influence operator, and only the second-order term remains in the equation of motion. Thus, although the present result has the identical form as the perturbative one, the restriction of the weak system–bath coupling can be eliminated. By taking the Markov limit in the resultant equation, we can obtain the Redfield equation. Hence, it is now clear that the Redfield equation actually has a wider scope of application than previously thought [42]. While this equation describes the exact dynamics of the density matrix, we found the serious limitations of this equation with respect to calculating an observable defined by a multi-time correlation function. This is because the present equation cannot describe the memory effects which straddle the operators involved in the correlation function due to the reduced description of the system. We demonstrate this point by calculating the third-order two-dimensional spectra from the present approach and from the QFP-LTC approach.

This paper is organized as follows. In Section 2, we derive the exact non-Markovian quantum master equation equivalent to the second-order TCL-QME by employing the path integral formalism. In Section 3, we briefly review the QFP-LTC formalism and discuss the limitation of the equation of motion derived in Section 2 by calculating third-order multidimensional spectra. Finally, Section 4 is devoted to concluding remarks.

2. Formulation

As a starting point, the total system is partitioned into a relevant system part (S) and the remaining bath degrees of freedom (B). The total Hamiltonian $\widehat{H}_{\rm tot}$ is then separated into a system part $\widehat{H}_{\rm S}$, a bath part $\widehat{H}_{\rm B}$, and the system–bath interaction $\widehat{H}_{\rm SB}$,

$$\widehat{H}_{\rm tot} = \widehat{H}_{\rm S} + \widehat{H}_{\rm B} + \widehat{H}_{\rm SB}. \tag{2.1}$$

The corresponding Liouvillian is decomposed as

$$\widehat{\mathscr{L}}_{\rm tot} = \widehat{\mathscr{L}}_{\rm S} + \widehat{\mathscr{L}}_{\rm B} + \widehat{\mathscr{L}}_{\rm SB}. \tag{2.2}$$

If necessary, the counter term $\widehat{H}_{\rm c}$ ($\widehat{\mathscr{L}}_{\rm c}$) can be added to the system part [43]. We assume that the bath degrees of freedom can be treated as an ensemble of harmonic oscillators as

$$\widehat{H}_{\rm B} = \sum_i \left[\frac{\hat{p}_i^2}{2} + \frac{\omega_i^2}{2}\hat{x}_i^2\right], \tag{2.3}$$

where x_i, p_i, and ω_i are the mass-weighted coordinate, conjugate momentum, and frequency of the ith bath oscillator, respectively. Unlike the real environment, there is no redistribution of energy within the present bath model since the bath modes are not coupled to each other. Furthermore, we assume that the bath coordinates are linearly coupled to the system,

$$\widehat{H}_{\rm SB} = -\widehat{V}_{\rm S}\sum_i c_i\hat{x}_i, \tag{2.4}$$

where $\widehat{V}_{\rm S}$ is an *arbitrary* dimensionless operator of the system and c_i denotes the coupling constant to the ith bath oscillator. Here, the system–bath coupling operator $V_{\rm S}$ does not necessarily commute with the system Hamiltonian.

Since we are only interested in the dynamics of the relevant system S, we eliminate the bath degrees of freedom leading to the reduced density matrix, $\hat{\rho}(t) \equiv \mathrm{Tr}_{\mathrm{B}}\{\hat{\rho}_{\mathrm{tot}}(t)\}$, i.e., the partial trace of the total density matrix over the bath degrees of freedom. This contains the information on the dynamic properties of the system influenced by the bath. While efforts have been made previously to include an initial quantum correlation (coherence) between the system and bath [26,44] we restrict our discussion to the case of the factorized initial condition defined by $\hat{\rho}_{\mathrm{tot}}(t_0) = \hat{\rho}(t_0)\hat{\rho}_{\mathrm{B}}^{\mathrm{eq}}$, where $\hat{\rho}_{\mathrm{B}}^{\mathrm{eq}}$ is the equilibrium density matrix of the bath alone. The effects of the correlation between the system and bath will be discussed in Section 3 in the context of a nonlinear optical response. To continue, $\hat{\rho}(t)$ evolves in time as follows:

$$\hat{\rho}^{(\mathrm{I})}(t) = \widehat{\mathscr{G}}^{(\mathrm{I})}(t;t_0)\hat{\rho}^{(\mathrm{I})}(t_0), \tag{2.5}$$

where the reduced propagator $\widehat{\mathscr{G}}(t;t_0)$ is given by

$$\widehat{\mathscr{G}}^{(\mathrm{I})}(t;t_0) \equiv \left\langle \mathrm{T}\exp\left(-\mathrm{i}\int_{t_0}^{t}\mathrm{d}s\,\widehat{\mathscr{L}}_{\mathrm{SB}}^{(\mathrm{I})}(s)\right)\right\rangle_{\mathrm{B}}. \tag{2.6}$$

Here, $\langle\cdots\rangle_{\mathrm{B}}$ stands for $\mathrm{Tr}_{\mathrm{B}}\{\cdots\hat{\rho}_{\mathrm{B}}^{\mathrm{eq}}\}$ and the symbol 'T' describes the usual chronological time ordering. For later convenience, we have employed the interaction picture for the Liouvillian without the system–bath interaction, $\widehat{\mathscr{L}}_0 \equiv \widehat{\mathscr{L}}_{\mathrm{S}} + \widehat{\mathscr{L}}_{\mathrm{B}}$. The superscript '(I)' indicates an operator in the interaction picture. Using the path integral formalism under the conditions Eqs. (2.3) and (2.4), we can derive an exact (nonperturbative and non-Markovian) expression for the propagator. For a representation $\hat{\varphi} \mid \varphi\rangle = \varphi \mid \varphi\rangle$ (e.g., $\hat{\varphi}$ is a coordinate operator $\hat{q}$ or an annihilation operator $\hat{a}$; φ is an eigenvalue of the operator $\hat{\varphi}$), the matrix element of the propagator can be expressed as [29–31,39]

$$\begin{aligned}&\langle\langle\varphi,\varphi';t|\widehat{\mathscr{G}}^{(\mathrm{I})}(t;t_0)|\varphi_0,\varphi_0';t_0\rangle\rangle\\ &\quad=\int_{(\varphi_0,t_0)}^{(\varphi,t)}\mathscr{D}\varphi\int_{(\varphi_0',t_0)}^{(\varphi',t)}\mathscr{D}\varphi'\mathrm{e}^{\mathrm{i}(S[\varphi]-S[\varphi'])/\hbar}\,\mathrm{e}^{-W[\varphi,\varphi']},\end{aligned} \tag{2.7}$$

where $S[\varphi]$ is the action corresponding to $\widehat{H}_S$, and $\mathrm{e}^{-W[\varphi,\varphi']}$ is the Feynman–Vernon influence functional, which encompasses the influence of the bath on the system. The influence phase $W[\varphi,\varphi']$ is explicitly given by

$$\begin{aligned}W[\varphi,\varphi'] = \frac{1}{\hbar^2}\int_{t_0}^{t}\mathrm{d}s\int_{t_0}^{s}\mathrm{d}u V_-(s)[C_{\mathrm{B}}'(s-u)V_-(u)\\ +\mathrm{i}C_{\mathrm{B}}''(s-u)V_+(u)],\end{aligned} \tag{2.8}$$

where $C_{\mathrm{B}}'(t)$ and $C_{\mathrm{B}}''(t)$ are the real and imaginary parts of the correlation function of the collective bath coordinate $\widehat{X}^{(I)}(t) \equiv \sum_i c_i\hat{x}_i^{(\mathrm{I})}(t)$,

$$C_{\mathrm{B}}(t) \equiv \langle\widehat{X}^{(\mathrm{I})}(t)\widehat{X}^{(\mathrm{I})}(0)\rangle_{\mathrm{B}}. \tag{2.9}$$

In the above, we have introduced the abbreviations,

$$V_-(t) \equiv V(\varphi(t)) - V(\varphi'(t)) \tag{2.10a}$$

and

$$V_+(t) \equiv V(\varphi(t)) + V(\varphi'(t)). \tag{2.10b}$$

Any time-ordered operator product, $\mathrm{T}\hat{\varphi}^{(I)}(t_1)\cdots\hat{\varphi}^{(I)}(t_n)$ $(t_{\mathrm{F}} > t_1,\ldots,t_n > t_{\mathrm{I}})$, can be incorporated as a function of time in the functional formalism and expressed as [45]

$$\begin{aligned}&\langle\varphi_{\mathrm{F}},t_{\mathrm{F}}|\mathrm{T}\hat{\varphi}^{(\mathrm{I})}(t_1)\cdots\hat{\varphi}^{(\mathrm{I})}(t_n)|\varphi_{\mathrm{I}},t_{\mathrm{I}}\rangle\\ &\quad=\int_{(\varphi_{\mathrm{I}},t_{\mathrm{I}})}^{(\varphi_{\mathrm{F}},t_{\mathrm{F}})}\mathscr{D}\varphi\;\mathrm{e}^{\mathrm{i}S[\varphi]/\hbar}\varphi(t_1)\cdots\varphi(t_n).\end{aligned} \tag{2.11}$$

In the operator representation, Eq. (2.7) is expressed as

$$\widehat{\mathscr{G}}^{(\mathrm{I})}(t;t_0) = \mathrm{T}\exp\left[-\int_{t_0}^{t}\mathrm{d}s\,\widehat{\mathscr{W}}^{(\mathrm{I})}(s)\right] \tag{2.12}$$

with

$$\begin{aligned}\widehat{\mathscr{W}}^{(\mathrm{I})}(s) = \frac{1}{\hbar^2}\int_{t_0}^{s}\mathrm{d}s'\,\widehat{V}^{(\mathrm{I})}(s)^{\times}[C_{\mathrm{B}}'(s-s')\widehat{V}^{(\mathrm{I})}(s')^{\times}\\ +\mathrm{i}C_{\mathrm{B}}''(s-s')\widehat{V}^{(\mathrm{I})}(s')^{\circ}],\end{aligned} \tag{2.13}$$

where we have introduced the hyper-operator notations $\hat{\mathscr{O}}^{\times}\hat{f} \equiv [\hat{\mathscr{O}},\hat{f}]$ and $\hat{\mathscr{O}}^{\circ}\hat{f} \equiv \{\hat{\mathscr{O}},\hat{f}\}$ for any operator $\hat{\mathscr{O}}$ and operand operator $\hat{f}$. Thus, we can obtain the following equation of motion,

$$\frac{\partial}{\partial t}\hat{\rho}^{(\mathrm{I})}(t) = -\hat{\mathscr{W}}^{(\mathrm{I})}(t)\hat{\rho}^{(\mathrm{I})}(t). \tag{2.14}$$

As can be seen from the definition of Eqs. (2.5) and (2.6), the operator $\hat{\rho}^{(\mathrm{I})}(t)$ is equivalent to the distribution function in the influence functional formalism and is the exact density operator which involves all orders of the system–bath interaction. Since we obtain the above equation of motion by simply carrying out the time derivative of the propagator Eq. (2.12), this equation describes the exact (i.e. nonperturbative and non-Markovian) dynamics of the reduced system. The key feature of this expression is the time-convolutionless expression of the influence phase operator $\widehat{\mathscr{W}}^{(\mathrm{I})}(t)$. The higher-order system–bath interaction at different time events can be taken into account by integrating Eq. (2.14). Thus, Eq. (2.14) allows us to evaluate the reduced density matrix element by means of a differential equation instead of functional integration.

Noting Eq. (2.4) and turning back to the Schrödinger picture, we can recast Eq. (2.14) into

$$\frac{\partial}{\partial t}\hat{\rho}(t) = -\mathrm{i}\widehat{\mathscr{L}}_{\mathrm{S}}\hat{\rho}(t) - \int_{t_0}^{t}\mathrm{d}s\langle\widehat{\mathscr{L}}_{\mathrm{SB}}\mathrm{e}^{-\mathrm{i}\widehat{\mathscr{L}}_0(t-s)}\widehat{\mathscr{L}}_{\mathrm{SB}}\mathrm{e}^{-\mathrm{i}\widehat{\mathscr{L}}_0(s-t)}\rangle_{\mathrm{B}}\hat{\rho}(t). \tag{2.15}$$

This equation coincides with the time-convolutionless quantum master equation (TCL-QME) developed by Shibata et al. [10,11] with the second-order perturbative approximation. From the time-convolution equation such as the Nakajima–Zwanzig identity [8,9], we can also obtain Eq. (2.15) by employing the approximation, $\hat{\rho}(t-\tau) \approx \mathrm{e}^{\mathrm{i}\widehat{\mathscr{L}}_S\tau}\hat{\rho}(t)$, in addition to the second-order perturbative approximation [18]. While the perturbative expression is obtained by expanding the propagator Eq. (2.6) in terms

of the system–bath coupling up to some order, we have obtained the present result by including all orders of the system–bath interaction. We were able to obtain the exact expression because we assumed a harmonic bath in employing the framework of the influence functional formalism. To illustrate the difference between the perturbative approach and the present one, we derived the perturbative results up to the fourth-order in Appendix. Since the second-order approximation coincides with the present exact result, the situation becomes ironic. While the second-order expression can give the exact result, the inclusion of the fourth-order interaction gives only approximate results that are valid only for weak system–bath interaction. If we include all orders of the perturbative expansion, their contributions to dynamics higher than the second-order interaction cancel. Although the present resultant expression, Eq. (2.15), is exactly the same as the second-order perturbative expression of the TCL-QME, it can handle a strong system–bath interaction in the case of colored noise. In order to address this point, we call Eq. (2.15) *the nonperturbative non-Markovian quantum master equation (NN-QME)*.

Up to this point, our argument is merely formal as a case of the Feynman–Vernon influence functional. To show its practical value as well as the limitation of the formalism, we assume that the system Hamiltonian is *time-independent* and employs the eigenstate representation, $\widehat{H}_{\rm S} \mid a\rangle = \hbar\omega_a \mid a\rangle$. Thus, Eq. (2.15) is evaluated as

$$\frac{\partial}{\partial t}\rho_{ab}(t) = -\mathrm{i}\omega_{ab}\rho_{ab}(t) + \sum_{c,d} R_{ab,cd}(t)\rho_{cd}(t), \tag{2.16}$$

where we have introduced the notations $\rho_{ab}(t) \equiv \langle a \mid \hat{\rho}(t) \mid b\rangle$ and $\omega_{ab} \equiv \omega_a - \omega_b$. The tetradic relaxation matrix $R_{ab,cd}(t)$ is expressed as

$$\begin{aligned} R_{ab,cd}(t) \equiv{}& \Gamma_{db,ac}(\omega_{ca};t) + \Gamma^*_{ca,bd}(\omega_{db};t) - \delta_{bd}\sum_e \Gamma_{ae,ec}(\omega_{ce};t) \\ & - \delta_{ac}\sum_e \Gamma^*_{be,ed}(\omega_{de};t) \end{aligned} \tag{2.17}$$

in terms of the damping matrix,

$$\Gamma_{ab,cd}(\omega_{dc};t) = \langle a \mid \widehat{V}_{\rm S} \mid b\rangle\langle c \mid \widehat{V}_{\rm S} \mid d\rangle \widetilde{C}_{\rm B}(\omega_{dc};t-t_0) \tag{2.18}$$

with the relaxation function,

$$\widetilde{C}_{\rm B}(\omega;t-t_0) \equiv \frac{1}{\hbar^2}\int_0^{t-t_0} \mathrm{d}s C_{\rm B}(s)\mathrm{e}^{\mathrm{i}\omega(-s)}. \tag{2.19}$$

This is the nonperturbative non-Markovian Redfield equation. The identical equation for non-Markovian noise has been derived from the second-order perturbative approach [18]. However, the result can be used for nonperturbative cases. In general, the bath correlation function $C_{\rm B}(t)$ decays to zero within a certain time scale $\tau_{\rm c}$, which depends on a set of bath parameters. In the time region, $t - t_0 > \tau_{\rm c}$, the upper integration limit in Eq. (2.19) can be replaced by infinity (the Markov limit). Then, Eq. (2.16) deduces to the conventional Redfield equation.

All information on the bath is contained in the spectral density function, $J(\omega) = \pi\sum_i [c_i^2/2\omega_i]\delta(\omega-\omega_i)$. We now specify the character of the bath by choosing $J(\omega)$. Several forms of the function are being employed in the literature, either based on model assumptions or analyses of molecular simulations. Here, we focus on the Ohmic spectral density with the Lorentz–Drude form,

$$J(\omega) = \frac{\hbar\zeta}{\omega_0}\omega\cdot\frac{\gamma^2}{\omega^2+\gamma^2}, \tag{2.20}$$

where ω_0 is a characteristic frequency of the relevant system. The parameters γ and ζ are related to the correlation time and the strength of noise by the bath, respectively [36]. Eq. (2.9) is then evaluated as

$$C_{\rm B}(t) = \mathrm{i}\frac{\hbar^2\zeta\gamma^2}{\omega_0} n_{\rm BE}(\mathrm{i}\gamma)\mathrm{e}^{-\gamma t} + \sum_{k=1}^{\infty}\frac{2\mathrm{i}}{\beta} J(\mathrm{i}\nu_k)\mathrm{e}^{-\nu_k t}, \tag{2.21}$$

where the quantities $n_{\rm BE}(\omega) \equiv 1/(\mathrm{e}^{\beta\hbar\omega}-1)$ and $\nu_k \equiv 2\pi k/\beta\hbar$ are the Bose–Einstein distribution function and the bosonic Matsubara frequency, respectively. In Eq. (2.21), the first term indicates that the bath oscillators disturb the relevant system with the colored noise, characterized by an exponential decay in the correlation. The additional terms involving the Matsubara frequencies imply a quantum effect of the bath-noise. At low-temperature characterized by $\beta\hbar\omega_0/2 \gtrsim 1$, the disregard of these terms destroys the quantum interference between the system and the bath, and then gives rise to an unphysical result known as *the positivity problem*, where the populations of the excited states become negative [36,39]. The time-integration in Eq. (2.19) can be performed analytically as follows:

$$\begin{aligned} \widetilde{C}_{\rm B}(\omega;t) = {}& \mathrm{i}\frac{\zeta\gamma^2}{\omega_0} n_{\rm BE}(\mathrm{i}\gamma)\frac{1-\mathrm{e}^{(\mathrm{i}\omega-\gamma)t}}{-\mathrm{i}\omega+\gamma} + \frac{1}{\hbar^2}\sum_{k=1}^{\infty}\frac{2\mathrm{i}}{\beta}J(\mathrm{i}\nu_k) \\ & \times\frac{1-\mathrm{e}^{(\mathrm{i}\omega-\nu_k)t}}{-\mathrm{i}\omega+\nu_k}, \end{aligned} \tag{2.22}$$

which is dominated not only by the noise correlation time $\tau_{\rm c} \equiv \gamma^{-1}$ but also by the Matsubara frequencies $\{\nu_k\}_{k=1}^{\infty}$. After the transient region, i.e. $t > \max(\gamma^{-1}, \nu_1^{-1})$, Eq. (2.22) reaches the stationary value $\widetilde{C}_{\rm B}(\omega;\infty)$ given by

$$\mathrm{Re}\widetilde{C}_{\rm B}(\omega;\infty) = \frac{J(\omega)}{\hbar}[n_{\rm BE}(\omega)+1] \tag{2.23a}$$

and

$$\begin{aligned} \mathrm{Im}\widetilde{C}_{\rm B}(\omega;\infty) = {}& -\frac{J(\omega)}{\hbar\pi}\left[\frac{\pi\gamma}{2\omega} + \frac{\pi}{\beta\hbar\gamma} + \psi\left(\frac{\beta\hbar\gamma}{2\pi}\right)\right. \\ & \left. -\mathrm{Re}\psi\left(\mathrm{i}\frac{\beta\hbar\omega}{2\pi}\right)\right], \end{aligned} \tag{2.23b}$$

where $\psi(z)$ is the digamma function defined in terms of the gamma function $\Gamma(z)$ as follows: $\psi(z) \equiv \mathrm{d}\ln\Gamma(z)/\mathrm{d}z$ [46].

In Eq. (2.23), the spectral density has been extended to negative frequencies via $J(-\omega) \equiv -J(\omega)$.

3. Discussion: limitation to calculate nonlinear response functions

Although the NN-QME correctly describes the dynamics of the reduced density matrix, there is a limitation in evaluating the nonlinear response function that is defined by multi-time correlation functions of system observables. To illustrate this point, we introduce the quantum Fokker–Planck equation with low-temperature correction terms (QFP-LTC) [39] that can also be used to study the dynamics nonperturbatively without employing the energy eigenstate representation of the system. Then we investigate the role of the correlation (quantum coherence) between the system and bath by calculating the third-order response function as two-dimensional spectra of ultrafast nonlinear optical measurements using the NN-QME given by Eq. (2.15) and the QFP-LTC equation.

For the spectral distribution Eq. (2.20), the QFP-LTC equation for the reduce density, $\hat{\rho}(\mathbf{0};t) \equiv \hat{\rho}(t)$, is given by

$$\frac{\partial}{\partial t}\hat{\rho}(\mathbf{j};t) = -\mathrm{i}\widehat{\mathscr{L}}_{\mathrm{S}}\hat{\rho}(\mathbf{j};t) - \left[\sum_{k=0}^{K} j_k \nu_k + \hat{\Xi}\right]\hat{\rho}(\mathbf{j};t) - \sum_{k=0}^{K}\hat{\Phi}\hat{\rho}(\mathbf{j}_{k+};t) - \sum_{k=0}^{K} j_k \nu_k \hat{\Theta}_k \hat{\rho}(\mathbf{j}_{k-};t), \tag{3.1}$$

where we have defined $\nu_0 \equiv \gamma$, and have introduced the $(K+1)$-dimensional vectors consisting of nonnegative integers, $\mathbf{j} \equiv (j_0, j_1, \ldots, j_K)$ and $\mathbf{j}_{k\pm} \equiv (j_0, \ldots, j_k \pm 1, \ldots, j_K)$. Here, it should be noted that only $\hat{\rho}(\mathbf{0};t) = \hat{\rho}(t)$ describes the dynamics to be measured. The other elements are the auxiliary operators being introduced in order to take into account such a correlation between the system and the bath as memory effects and quantum interference. The value of K is determined so as to satisfy the condition,

$$\nu_K \gg \omega_0. \tag{3.2}$$

The bath-induced relaxation operators are defined by

$$\hat{\Phi} \equiv \mathrm{i}\widehat{V}^{\times}, \tag{3.3a}$$

$$\hat{\Theta}_0 \equiv \mathrm{i}\frac{\zeta}{\beta\hbar\omega_0}[z\cot z\,\widehat{V}^{\times} - \mathrm{i}z\widehat{V}^{\circ}], \tag{3.3b}$$

$$\hat{\Theta}_k \equiv \mathrm{i}\frac{\zeta}{\beta\hbar\omega_0}\frac{2z^2}{\pi^2k^2 - z^2}\widehat{V}^{\times}\ (k \geqslant 1), \tag{3.3c}$$

and

$$\hat{\Xi} \equiv \sum_{k=1}^{K}\hat{\Phi}\hat{\Psi}_k + \frac{\zeta}{\beta\hbar\omega_0}(1 - z\cot z)\widehat{V}^{\times}\widehat{V}^{\times} \tag{3.3d}$$

with $z \equiv \beta\hbar\gamma/2$. The hierarchically coupled equations, Eq. (3.1), continue to infinity, which is impractical to solve numerically. To terminate the equations at the finite stages, we introduce the terminator as follows [39]:

$$\frac{\partial}{\partial t}\hat{\rho}(\mathbf{j};t) \simeq -\mathrm{i}\hat{\mathscr{L}}_{\mathrm{S}}\hat{\rho}(\mathbf{j};t) - \hat{\Xi}\hat{\rho}(\mathbf{j};t), \tag{3.4}$$

which is valid for the nonnegative integers $j_0, j_1, \ldots, j_K$ satisfying

$$N \equiv \sum_{k=0}^{K} j_k \gg \frac{\omega_0}{\min(\nu_0 = \gamma, \nu_1)}. \tag{3.5}$$

In practice, we may use the lower values of K and N, both of which do not satisfy Eqs. (3.2) and (3.5), respectively. The numerical implementation of the formulation is not as cumbersome as it appears to be. Since the bath-induced relaxation operators in Eq. (3.3) are all time-independent as opposed to those in Eq. (2.16), the time integration of the equations of motion is straightforward.

As long as we consider relaxation processes of the reduced density operator, the QFP-LTC and the NN-QME are equivalent to each other. In order to verify this, the diagrammatic expressions for the reduced density operator, Eq. (2.12), is represented in Fig. 1. Each diagram corresponds to an expanded term of the time-ordered exponential operator of the system–bath interaction. The solid lines represent a free time-evolution of a reduced density, whereas the broken lines represent a bath-phonon absorption–emission process corresponding to $C_{\mathrm{B}}(s_j - u_j)$. During the time-evolution of the reduced operator, the phonon absorption–emission processes occur repetitively. If we observe the state of the system at time t, all excited phonons relax because of the trace of the expectation value defined by $\langle\widehat{A}(t)\rangle = \mathrm{Tr}_{\mathrm{tot}}\{\widehat{A}\hat{\rho}_{\mathrm{tot}}(t)\} = \mathrm{Tr}_{\mathrm{S}}\{\widehat{A}\hat{\rho}(t)\}$ for the system operator $\widehat{A}$. In the QFP-LTC formalism, the states are described just by the operator $\hat{\rho}(t) = \hat{\rho}(\mathbf{0};t)$. The other hierarchical members $\hat{\rho}(\mathbf{j} \neq \mathbf{0};t)$, which are certainly missing in the NN-QME, do not play any roles for the measurement at time t.

The significance of the hierarchical members, or the superiority of the QFP-LTC formalism becomes evident when we consider multi-time correlation functions of physical observables. In nonlinear spectroscopic experiments including off-resonant and resonant multidimensional spectroscopy [47,48], the signals are described by the nonlinear response function characterized by the multi-time correlation functions of the optical dipole $\hat{\mu}$ or the polarization

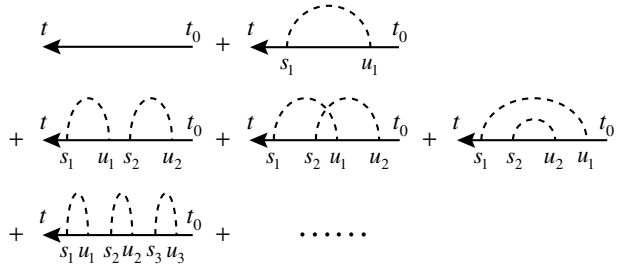

Fig. 1. Diagrammatic expressions for a time-evolution of the reduced density operator $\hat{\rho}(t)$ propagated by Eq. (2.12). A solid line represents a free time-evolution of a reduced density, whereas a broken line represents a bath-phonon absorption–emission process corresponding to $C_{\mathrm{B}}(s_j - u_j)$.

$\hat{\alpha}$ in the systems of interest [49]. Here, we consider the third-order nonlinear response function expressed as

$$R^{(3)}(t;t_3,t_2,t_1) \equiv \left(\frac{\mathrm{i}}{\hbar}\right)^3 \mathrm{Tr}_{\mathrm{tot}}\{\mu(t)\mu(t_3)^{\times}\mu(t_2)^{\times}\mu(t_1)^{\times}\hat{\rho}_{\mathrm{tot}}(t_0)\}, \tag{3.6}$$

where $\hat{\mu}(t) \equiv \mathrm{e}^{\mathrm{i}\widehat{H}_{\mathrm{tot}}t/\hbar}\hat{\mu}\mathrm{e}^{-\mathrm{i}\widehat{H}_{\mathrm{tot}}t/\hbar}$ is the Heisenberg representation of $\hat{\mu}$. Through the reduction procedure, Eq. (3.6) can be recast into

$$R^{(3)}(t;t_3,t_2,t_1) = \left(\frac{\mathrm{i}}{\hbar}\right)^3 \mathrm{Tr}_{\mathrm{S}}\{\mu^{(\mathrm{I})}(t)\hat{\sigma}^{(\mathrm{I})}(t;t_3,t_2,t_1)\}, \tag{3.7}$$

with

$$\hat{\sigma}^{(\mathrm{I})}(t;t_3,t_2,t_1) \equiv \mathrm{T}\mu^{(\mathrm{I})}(t_3)^{\times}\mu^{(\mathrm{I})}(t_2)^{\times}\mu^{(\mathrm{I})}(t_1)^{\times} \times \exp\left[-\int_{t_0}^{t}\mathrm{d}s\,\widehat{\mathscr{W}}^{(\mathrm{I})}(s)\right]\hat{\rho}(t_0). \tag{3.8}$$

Notice that the position of the symbol 'T' is different from that in Eq. (2.12). In Fig. 2, we show two representative diagrammatic expressions of the terms involved in Eq. (3.8). In the diagram (a), the states at time t_1, t_2, and t_3 are described by $\hat{\rho}(\mathbf{0};t_n) = \hat{\rho}(t_n)$ since all phonons relax at the points of the system–laser interaction. Thus, the phonon propagation can be factorized at these points. In the diagram (b), in contrast, the phonon propagation straddles the evolution ($t_1 \sim t_2$), waiting ($t_2 \sim t_3$), and detection ($t_3 \sim t$) periods. We term such time evolutions *the straddling evolutions*. As shown from the functional integral approach [50], the straddle evolutions illustrated by Fig. 2(b) closely relate to the quantum coherence between the system and bath and cannot be neglected for an accurate description of nonlinear response functions. Obviously, the states at time t_1, t_2, and t_3 in the diagram (b) cannot be described by the operator $\hat{\rho}(\mathbf{0};t_n) = \hat{\rho}(t_n)$ itself. The other hierarchical elements $\hat{\rho}(\mathbf{j} \neq \mathbf{0};t_n)$ defined in the interaction picture as

$$\hat{\rho}^{(\mathrm{I})}(\mathbf{j};t_n) \equiv \mathrm{T}\prod_{k=0}^{K}\left[-\int_{t_0}^{t_n}\mathrm{d}s\mathrm{e}^{-\nu_k(t_n-s)}\nu_k\hat{\Theta}_k^{(\mathrm{I})}(s)\right]^{j_k} \times \exp\left[-\int_{t_0}^{t_n}\mathrm{d}s\,\widehat{\mathscr{W}}^{(\mathrm{I})}(s)\right]\hat{\rho}^{(\mathrm{I})}(t_0) \tag{3.9}$$

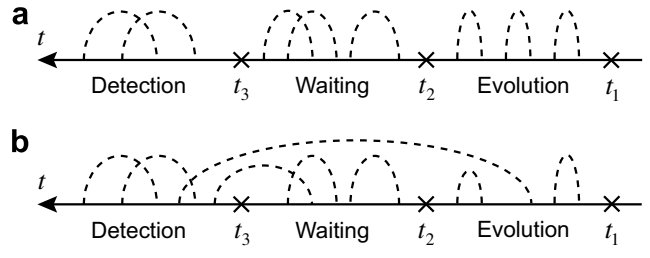

Fig. 2. Diagrammatic expressions of the system–bath interaction involved in the third-order nonlinear response function, Eqs. (3.7) and (3.8). The cross stands for the system–laser interaction associated with the operator $\hat{\mu}^{(\mathrm{I})}(t_n)^{\times}$. In (a), the phonon propagations are factorized by the system–laser interaction. In (b), in contrast, the phonon propagations straddle the three periods, the evolution period ($t_1 \sim t_2$), the waiting period ($t_2 \sim t_3$), and the detection period ($t_3 \sim t$).

are necessary to include the equations of motion to describe the straddling evolutions. The above elements describe the density operator that is associated with the $\sum_{k=0}^{K} j_k$ phonons emitted in the time period between t_0 and t_n via the operators $\{\hat{\Theta}_k^{(\mathrm{I})}(s)\}_{k=0}^{K}$. (As can be seen from the form of Eq. (3.1), the operator $\hat{\Phi}$ corresponds to the phonon absorption processes. See Appendix A in Ref. [51].) While the QFP-LTC equation can handle the straddle evolutions through the laser interactions, the NN-QME, Eq. (2.15) cannot treat such dynamics, since this equation cannot describe the memory effects which straddle the system–laser interaction despite its non-Markovian character. Thus, although the present NN-QME accurately describes the time-evolution of the density operator, it cannot produce the nonlinear signals including multidimensional signals appropriately.

In order to demonstrate the limitation of the NN-QME, we present two-dimensional (2D) optical spectra calculated from two different formalisms. For simplicity, here, we treat a two-level system (TLS) whose Hamiltonian is expressed as

$$\widehat{H}_{\mathrm{S}} = \frac{\hbar\omega_0}{2}\sigma_z, \tag{3.10}$$

where σ_j is a jth component ($j = x, y, z$) of the Pauli matrix. The system–bath coupling operator $\widehat{V}_{\mathrm{S}}$ in Eq. (2.4) is set to be in the form,

$$\widehat{V}_{\mathrm{S}} = \sigma_x + \frac{1}{2}\sigma_z, \tag{3.11}$$

where the inelastic part σ_x is responsible for the longitudinal (T_1-type) and transversal (T_2-type) relaxation processes in the TLS, whereas the elastic part σ_z induces the pure dephasing (T_2^*-type) process. Furthermore, we assume that the optical dipole $\hat{\mu}$ can be expressed as

$$\hat{\mu} = \sigma_x. \tag{3.12}$$

We calculate the rephasing (echo) response functions,

$$R_{\mathrm{R}}(\tau_3,\tau_2,\tau_1) \equiv -\mathrm{Tr}\left\{\hat{\mu}\widehat{G}(\tau_3)\frac{\mathrm{i}}{\hbar}\hat{\mu}_{\rightarrow}^{\times}\widehat{G}(\tau_3)\frac{\mathrm{i}}{\hbar}\hat{\mu}_{\rightarrow}^{\times}\widehat{G}(\tau_3)\frac{\mathrm{i}}{\hbar}\hat{\mu}_{\leftarrow}^{\times}\hat{\rho}_{\mathrm{tot}}^{\mathrm{eq}}\right\}, \tag{3.13}$$

and a nonrephasing (virtual echo) response function,

$$R_{\mathrm{NR}}(\tau_3,\tau_2,\tau_1) \equiv -\mathrm{Tr}\left\{\hat{\mu}\widehat{G}(\tau_3)\frac{\mathrm{i}}{\hbar}\hat{\mu}_{\rightarrow}^{\times}\widehat{G}(\tau_3) \times\frac{\mathrm{i}}{\hbar}\hat{\mu}_{\leftarrow}^{\times}\widehat{G}(\tau_3)\frac{\mathrm{i}}{\hbar}\hat{\mu}_{\rightarrow}^{\times}\hat{\rho}_{\mathrm{tot}}^{\mathrm{eq}}\right\}, \tag{3.14}$$

where $\widehat{G}(\tau)$ is the retarded propagator of the total system in the Liouville space, and $\tau_1 \equiv t_2 - t_1$, $\tau_2 \equiv t_3 - t_2$, and $\tau_3 \equiv t - t_3$. In the above, we have introduced the following operators [40,41],

$$\hat{\mu}_{\rightleftarrows} \equiv \frac{\sigma_x \pm \mathrm{i}\sigma_y}{2}. \tag{3.15}$$

By carrying out the double Fourier transform of Eqs. (3.13) and (3.14) with respect to τ_1 and τ_3, the 2D rephasing and nonrephasing spectra are, respectively, given by

$$S_{\mathrm{R}}(\Omega_3,\Omega_1;\tau_2) \equiv \mathrm{Im}\int_0^\infty \mathrm{d}\tau_3 \mathrm{e}^{\mathrm{i}\Omega_3\tau_3}\int_0^\infty \mathrm{d}\tau_1 \mathrm{e}^{\mathrm{i}\Omega_1\tau_1} R_{\mathrm{R}}(\tau_3,\tau_2,\tau_1) \tag{3.16}$$

and

$$S_{\mathrm{NR}}(\Omega_3,\Omega_1;\tau_2) \equiv \mathrm{Im}\int_0^\infty \mathrm{d}\tau_3 \mathrm{e}^{\mathrm{i}\Omega_3\tau_3}\int_0^\infty \mathrm{d}\tau_1 \mathrm{e}^{\mathrm{i}\Omega_1\tau_1} R_{\mathrm{NR}}(\tau_3,\tau_2,\tau_1). \tag{3.17}$$

The individual 2D rephasing and nonrephasing spectra show distorted line shapes, the so-called phase-twisted lines, because the double Fourier transform leads to a combination of absorptive and dispersive features [52]. By adding the 2D rephasing and nonrephasing spectra in equal weights, however, we can cancel out the dispersive contribution so that we can obtain the 2D correlation spectrum with only the absorptive line shape [53]

$$S_{\mathrm{c}}(\Omega_3,\Omega_1;\tau_2) \equiv S_{\mathrm{R}}(\Omega_3,-\Omega_1;\tau_2) + S_{\mathrm{NR}}(\Omega_3,\Omega_1;\tau_2). \tag{3.18}$$

For numerical calculations, we set the system–bath parameters in Eqs. (2.22) and (3.3) as follows: $\omega_0 = 2100\,\mathrm{cm}^{-1}$, $\zeta = 0.5\omega_0$, $\gamma = 0.005\omega_0$, and $\beta\hbar\omega_0 = 10$. Because the value of γ is quite small compared with that of ω_0, the non-Markovian memory effect is significant in the system. With respect to calculating Eqs. (3.13) and (3.14) numerically, refer to Refs. [40,41].

Fig. 3 presents the 2D correlation spectra calculated from the two formalisms, (a) the NN-QME and (b) the QFP-LTC, for different waiting times, τ_2. The 2D correlation spectra in the panel (a) show completely different characteristics from the those in the panel (b). In the panel (b), the 2D-lineshape at $\tau_2 = 0$ is elongated along the diagonal line. This elongation is the evidence of correlation due to the straddling evolution between the evolution period ($t_1 \sim t_2$) and the detection period ($t_3 \sim t$) [54–56]. We can see that the higher-frequency part (the upper right portion) of the ellipse-like lineshape is slightly broadened compared with the lower-frequency part (the lower left portion). This phenomenon is caused by the cross-term contribution between the inelastic (σ_x) and elastic (σ_z) interactions which is known as the bath-induced *conversion between coherence to population* process [34,51,57]. With the increase in the value of τ_2, the degree of the elongation is dwindling. During the waiting period ($t_2 \sim t_3$), the correlation is destroyed by the fluctuation–dissipation processes, so that the memory is faded by the elapse of the waiting time τ_2. The behavior of the 2D-lineshape in the panel (b) has been observed experimentally [56,58,59]. On the other hand, the 2D-lineshape at $\tau_2 = 0$ in the panel (a) does not show the elongation; it has the star-like characteristic. The characteristic is observed in the fast bath-noise correlation cases, where the correlation between the evolution and detection periods is vanishingly small [56]. Furthermore, the 2D-lineshape in panel (a) is elongating along the Ω_3 axis direction with an increase in the value of τ_2. These are artifacts caused by the above-mentioned limitation of the NN-QME, and hence the 2D-lineshapes in the panel (a) have no physical meaning. The validity of the NN-QME to calculate nonlinear response functions is limited to the fast bath-noise case, where the quantum coherence between the system and bath plays a minor role.

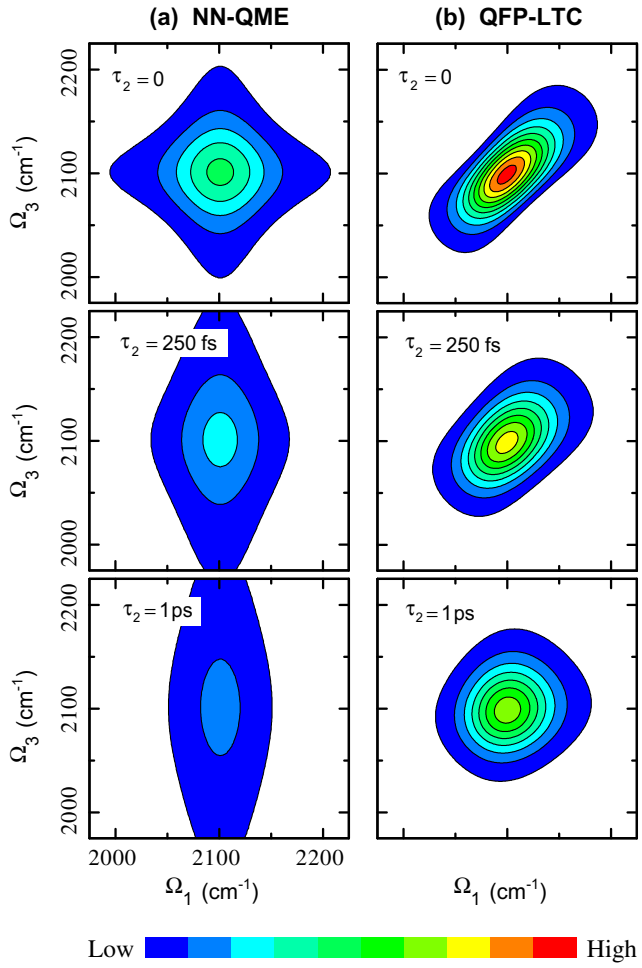

Fig. 3. 2D correlation spectra, $S_C^{(3)}(\Omega_3,\Omega_1;\tau_2)$, for the two-level system whose characteristic frequency is $\omega_0 = 2100\,\mathrm{cm}^{-1}$. The spectra were calculated from (a) the NN-QME approach with Eq. (2.16) and (b) the QFP-LTC approach with Eq. (3.1). For both approaches, the system–bath parameters are set to be $\zeta = 0.5\omega_0$, $\gamma = 0.005\omega_0$, and $\beta\hbar\omega_0 = 10$. The normalization of the 2D spectra is such that the maximum at $\tau_2 = 0$ in the panel (b) is unity. Ten equally spaced contour levels from 0.05 to 0.95 are drawn for each plot.

4. Concluding remarks

Assuming the harmonic oscillator heat bath and the factorized initial condition, we have derived a nonperturbative non-Markovian quantum master equation (NN-QME) for a reduced density operator. We have found that the resultant expression coincides with the second-order approximation form of the TCL-QME. This result indicates that the effects of higher-order system–bath interactions can be incorporated into the influence operator as given in Eq. (2.13) and that contributions higher than the second-order do not play any role once we sum up all contribu-

tions. By employing the energy eigenstate representation, we reduced the above approach to the nonperturbative non-Markovian Redfield equation, which also coincides with the generalized Redfield equation derived for a weak system–bath interaction. Our derivation of the Redfield equation indicates that the equation actually has a wider scope of application than previously thought. While the presently derived equation, the NN-QME, is valid under the assumption of the factorized initial condition, this approach can describe the time-evolution of the density operator for any spectral distribution at any temperature of the bath. As long as the system Hamiltonian is time-independent and the factorization assumption is relevant, the present approach has advantages in evaluating the time-evolution of the density matrix elements in comparison to the QFP-LTC approach.

If we need to calculate nonlinear response functions, however, the NN-QME formalism can be applied only for fast bath-noise correlation cases. This is because the NN-QME cannot handle the correlations between the system and the bath depicted as the straddling evolution of the bath phonons. The fact also restricts the NN-QME approach to calculations of the time evolution of density matrix elements under time-dependent external forces. In such situations, we encounter the difficulty not only to include the system–bath coherence but also to employ the energy eigenstate representation of the system, which is necessary to derive the time-dependent relaxation matrices in the Redfield equation.

Although the form of the spectral distribution is restricted to Eq. (2.20), the QFP-LTC formalism can handle a variety of systems including systems with time-dependent external forces. The formalism can also treat systems defined in coordinate space with the effects of the correlated initial condition. [31,32,39]. Thus, the validity and limitation of the NN-QME for a general spectral distribution may be justified by comparing the results obtained from the QFP-LTC.

End note

The reviewer informed us that a similar work by R. Doll, et al. appeared on the preprint server (http://arxiv.org/abs/0707.3938) about the same time we submitted our manuscript. While their result was limited to the dephasing case, our result was for a general system–bath interaction. A role of the quantum coherence between the system and bath was also discussed as the context of nonlinear response functions.

Acknowledgements

A.I. appreciates the support of Research Fellowships of the Japan Society for the Promotion of Science for Young Scientists, No.18-2691. Y.T. is grateful for the financial support of Grant-in-Aid for Scientific Research B19350011 from the Japan Society for the Promotion of Science.

Appendix.

We derive a time-convolutionless quantum master equation from the conventional perturbative approach up to the fourth-order to illustrate the difference from the nonperturbative approach.

The reduced propagator Eq. (2.6) can be expanded as follows:

$$\widehat{\mathscr{G}}^{(\mathrm{I})}(t;t_0)=\sum_{n=0}^{\infty}g^{2n}\widehat{M}_{2n}(t), \tag{A.1}$$

where we have defined the nth-order moment as

$$g^n\widehat{M}_n(t)\equiv(-\mathrm{i})^n\int_{t_0}^{t}\mathrm{d}t_1\int_{t_0}^{t_1}\mathrm{d}t_2\ldots\int_{t_0}^{t_{n-1}}\mathrm{d}t_n \times\langle\widehat{\mathscr{L}}_{\mathrm{SB}}^{(\mathrm{I})}(t_1)\widehat{\mathscr{L}}_{\mathrm{SB}}^{(\mathrm{I})}(t_2),\ldots,\widehat{\mathscr{L}}_{\mathrm{SB}}^{(\mathrm{I})}(t_n)\rangle_{\mathrm{B}}. \tag{A.2}$$

In Eq. (A.1), the terms of odd powers in $\widehat{\mathscr{L}}_{\mathrm{SB}}$ have vanished, because $\widehat{\mathscr{L}}_{\mathrm{SB}}$ is linear in the bath coordinates.

By truncating the propagator Eq. (A.1) up to second-order, we have

$$\hat{\rho}_2^{(\mathrm{I})}(t)=[1+g^2\widehat{M}_2(t)]\hat{\rho}(t_0)\equiv\widehat{\mathscr{U}}_2(t;t_0)\hat{\rho}(t_0), \tag{A.3}$$

where the subscript '2' of the $\hat{\rho}^{(\mathrm{I})}(t)$ stands for the density operator under the second-order perturbative approximation. By taking the time derivative of Eq. (A.3), we obtain the equation of motion for $\hat{\rho}_2^{(\mathrm{I})}(t)$ as

$$\frac{\partial}{\partial t}\hat{\rho}_2^{(\mathrm{I})}(t)=\widehat{\mathscr{K}}_2(t)\hat{\rho}_2^{(\mathrm{I})}(t) \tag{A.4}$$

with

$$\widehat{\mathscr{K}}_2(t)\equiv\partial_t\widehat{\mathscr{U}}_2(t;t_0)\cdot\widehat{\mathscr{U}}_2^{-1}(t;t_0), \tag{A.5}$$

where we have introduced the notation $\partial_t\equiv\partial/\partial t$. Within the second-order approximation, the operator $\widehat{\mathscr{K}}_2(t)$ can be evaluated as follows:

$$\widehat{\mathscr{K}}_2(t)=[\partial_t g^2\widehat{M}_2(t)][1+g^2\widehat{M}_2(t)]^{-1}\simeq g^2\partial_t\widehat{M}_2(t). \tag{A.6}$$

The second-order expression in Eq. (A.4) and the NN-QME in the interaction picture have the same form. However, $\hat{\rho}_2(t)$ in Eq. (A.3) involves only the 0th and second-order system–bath interaction (only the upper two diagrams in Fig. 1.), whereas $\rho(t)$ in the NN-QME contains all orders (all diagrams in Fig. 1) as defined by Eq. (2.6) with the influence operator Eq. (2.13). Thus, for the perturbative case, there exists the fourth-order correction denoted by the middle three diagrams in Fig. 1. For the fourth-order perturbation case, $\hat{\rho}_4(t)$, the equation of motion can be derived as follows:

$$\frac{\partial}{\partial t}\hat{\rho}_4^{(\mathrm{I})}(t)=\widehat{\mathscr{K}}_4(t)\hat{\rho}_4^{(\mathrm{I})}(t) \tag{A.7}$$

with

$$\widehat{\mathscr{K}}_4(t)\simeq g^2\partial_t\widehat{M}_2(t)+g^4[\partial_t\widehat{M}_4(t)-\partial_t\widehat{M}_2(t)\cdot\widehat{M}_2(t)]. \tag{A.8}$$

The second term of the right-hand side in Eq. (A.8) is the fourth-order correction for the second-order perturbation, which can be explicitly expressed as

$$\begin{aligned}\int_{t_0}^{t} \mathrm{d}t_1 \int_{t_0}^{t_1} \mathrm{d}t_2 \int_{t_0}^{t_2} \mathrm{d}t_3 \Big[& \langle \widehat{\mathscr{L}}_{\mathrm{SB}}^{(\mathrm{I})}(t) \widehat{\mathscr{L}}_{\mathrm{SB}}^{(\mathrm{I})}(t_1) \widehat{\mathscr{L}}_{\mathrm{SB}}^{(\mathrm{I})}(t_2) \widehat{\mathscr{L}}_{\mathrm{SB}}^{(\mathrm{I})}(t_3) \rangle_{\mathrm{B}} \\ & - \langle \widehat{\mathscr{L}}_{\mathrm{SB}}^{(\mathrm{I})}(t) \widehat{\mathscr{L}}_{\mathrm{SB}}^{(\mathrm{I})}(t_1) \rangle_{\mathrm{B}} \langle \widehat{\mathscr{L}}_{\mathrm{SB}}^{(\mathrm{I})}(t_2) \widehat{\mathscr{L}}_{\mathrm{SB}}^{(\mathrm{I})}(t_3) \rangle_{\mathrm{B}} \\ & - \langle \widehat{\mathscr{L}}_{\mathrm{SB}}^{(\mathrm{I})}(t) \widehat{\mathscr{L}}_{\mathrm{SB}}^{(\mathrm{I})}(t_2) \rangle_{\mathrm{B}} \langle \widehat{\mathscr{L}}_{\mathrm{SB}}^{(\mathrm{I})}(t_1) \widehat{\mathscr{L}}_{\mathrm{SB}}^{(\mathrm{I})}(t_3) \rangle_{\mathrm{B}} \\ & - \langle \widehat{\mathscr{L}}_{\mathrm{SB}}^{(\mathrm{I})}(t) \widehat{\mathscr{L}}_{\mathrm{SB}}^{(\mathrm{I})}(t_3) \rangle_{\mathrm{B}} \langle \widehat{\mathscr{L}}_{\mathrm{SB}}^{(\mathrm{I})}(t_1) \widehat{\mathscr{L}}_{\mathrm{SB}}^{(\mathrm{I})}(t_2) \rangle_{\mathrm{B}} \Big]. \end{aligned} \tag{A.9}$$

Once we sum up the contributions from all orders of the system–bath interaction, we can include them into a part of the density operator as the influence operator. This indicate that even if we include all orders of the relaxation operators in the Redfield equation, their contributions will be exactly canceled except the contribution from the second-order operator.

References

[1] R.E. Wyatt, J.Z.H. Zhang (Eds.), Dynamics of Molecules and Chemical Reactions, Marcel Dekker Inc., New York, 1996.
[2] T. Yamamoto, S. Kato, J. Chem. Phys. 112 (2000) 8006.
[3] B.J. Berne, G. Cicotti, D.F. Coker (Eds.), Classical and Quantum Dynamics in Condensed Phase Simulations, World Scientific, Singapore, 1998.
[4] R. Kapral, G. Ciccotti, J. Chem. Phys. 110 (1999) 8919.
[5] H. Wang, M. Thoss, W.H. Miller, J. Chem. Phys. 115 (2001) 2979.
[6] M. Thoss, H. Wang, W.H. Miller, J. Chem. Phys. 115 (2001) 2991.
[7] A.L. Kuzemsky, Intern. J. Modern. Phys. B 21 (2007) 2821.
[8] S. Nakajima, Prog. Theor. Phys. 20 (1958) 948.
[9] R. Zwanzig, J. Chem. Phys. 33 (1960) 1338.
[10] F. Shibata, Y. Takahashi, N. Hashitsume, J. Stat. Phys. 17 (1977) 171.
[11] S. Chaturvedi, F. Shibata, Z. Phys. B 35 (1979) 297.
[12] A.G. Redfield, Adv. Magn. Reson. 1 (1965) 1.
[13] J.M. Jean, R.A. Friesner, G.R. Fleming, J. Chem. Phys. 96 (1992) 5827.
[14] W.T. Pollard, R.A. Friesner, J. Chem. Phys. 100 (1994) 5054.
[15] O. Kühn, V. May, M. Schreiber, J. Chem. Phys. 101 (1994) 10404.
[16] J.M. Jean, G.R. Fleming, J. Chem. Phys. 103 (1995) 2092.
[17] D. Egorova, A. Kühl, W. Domcke, Chem. Phys. 268 (2001) 105.
[18] D. Egorova, M. Thoss, W. Domcke, H. Wang, J. Chem. Phys. 119 (2003) 2761.
[19] A. Kühl, W. Domcke, Chem. Phys. 259 (2000) 227.
[20] A. Kühl, W. Domcke, J. Chem. Phys. 116 (2002) 263.
[21] S. Hahn, G. Stock, J. Chem. Phys. 116 (2002) 1085.
[22] B. Balzer, S. Hahn, G. Stock, Chem. Phys. Lett. 379 (2003) 351.
[23] O. Kühn, V. Sundström, J. Phys. Chem. B 101 (1997) 3432.
[24] O. Kühn, V. Sundström, J. Chem. Phys. 107 (1997) 4154.
[25] B.B. Laird, J. Budimir, J.L. Skinner, J. Chem. Phys. 94 (1991) 4391.
[26] T.M. Chang, J.L. Skinner, Physica A 193 (1993) 483.
[27] D.R. Reichman, R.J. Silbey, J. Chem. Phys. 104 (1996) 1506.
[28] S. Jang, J. Cao, R.J. Silbey, J. Chem. Phys. 116 (2002) 2705.
[29] R.P. Feynman, F.L. Vernon, Ann. Phys. (N.Y.) 24 (1963) 118.
[30] A.O. Caldeira, A.J. Leggett, Physica A 121 (1983) 587.
[31] Y. Tanimura, R. Kubo, J. Phys. Soc. Jpn. 58 (1989) 101.
[32] Y. Tanimura, P.G. Wolynes, Phys. Rev. A 43 (1991) 4131.
[33] Y. Tanimura, T. Steffen, J. Phys. Soc. Jpn. 69 (2000) 4095.
[34] T. Kato, Y. Tanimura, J. Chem. Phys. 117 (2002) 6221.
[35] T. Kato, Y. Tanimura, J. Chem. Phys. 120 (2004) 260.
[36] Y. Tanimura, J. Phys. Soc. Jpn. 75 (2006) 082001.
[37] R. Kubo, Adv. Chem. Phys. 15 (1969) 101.
[38] Y. Tanimura, Phys. Rev. A 41 (1990) 6676.
[39] A. Ishizaki, Y. Tanimura, J. Phys. Soc. Jpn. 74 (2005) 3131.
[40] A. Ishizaki, Y. Tanimura, J. Chem. Phys. 125 (2006) 084501.
[41] A. Ishizaki, Y. Tanimura, J. Phys. Chem. A 111 (2007) 9269.
[42] A.M. Walsh, R.D. Coalson, Chem. Phys. Lett. 198 (1992) 293.
[43] U. Weiss, Quantum Dissipative Systems, Second ed., Wold Scientific, Singapore, 1999.
[44] H. Grabert, P. Schramm, G.-L. Ingold, Phys. Rep. 168 (1988) 115.
[45] B. Sakita, Quantum Theory of Many-variable Systems and Fields, World Scientific, Singapore, 1985.
[46] M. Abramowitz, I.A. Stegun, Handbook of Mathematical Functions, with Formulas, Graphs, and Mathematical Tables, Dover Publications, New York, 1964.
[47] Y. Tanimura, S. Mukamel, J. Chem. Phys. 99 (1993) 9496.
[48] Y. Tanimura, K. Okumura, J. Chem. Phys. 106 (1997) 2078.
[49] S. Mukamel, Principles of Nonlinear Optical Spectroscopy, Oxford University Press, 1995.
[50] Y. Tanimura, S. Mukamel, J. Phys. Chem. 97 (1993) 12596.
[51] A. Ishizaki, Y. Tanimura, J. Chem. Phys. 123 (2005) 014503.
[52] R.R. Ernst, G. Bodenhausen, A. Wokaun, Principles of Nuclear Magnetic Resonance in One and Two Dimensions, Oxford University Press, 1990.
[53] M. Khalil, N. Demirdoven, A. Tokmakoff, Phys. Rev. Lett. 90 (2003) 047401.
[54] K. Okumura, A. Tokmakoff, Y. Tanimura, Chem. Phys. Lett. 314 (1999) 488.
[55] A. Tokmakoff, J. Phys. Chem. A 104 (2000) 4247.
[56] M. Khalil, N. Demirdoven, A. Tokmakoff, J. Phys. Chem. A 107 (2003) 5258.
[57] O. Kühn, Y. Tanimura, J. Chem. Phys. 119 (2003) 2155.
[58] S. Woutersen, P. Hamm, J. Phys.: Condens. Matter. 14 (2002) R1035.
[59] J.B. Asbury, T. Steinel, C. Stromberg, S.A. Corcelli, C.P. Lawrence, J.L. Skinner, M.D. Fayer, J. Phys. Chem. A 108 (2004) 1107.